JOURNAL OF GEOPHYSICAL RESEARCH, VOL. 96, NO. D2, PAGES 2995–3011, FEBRUARY 20, 1991

Ozone and Other Trace Gases in the Arctic and Antarctic Regions: Three-Dimensional Model Simulations

CLAIRE GRANIER[1] AND GUY BRASSEUR

National Center for Atmospheric Research, Boulder, Colorado

A three-dimensional mechanistic model of the middle atmosphere with calculated dynamics and chemistry (*Rose and Brasseur*, 1989) is used to study the behavior of chemically active trace gases at high latitudes in winter and spring, and to simulate the formation of an ozone hole in Antarctica. The dynamics of both hemispheres is simulated by applying at the lower boundary of the model (8.5 km) a wavelike perturbation representing qualitatively a climatological tropospheric forcing. The chemical heterogeneous processes converting chlorine reservoirs into active chlorine in cold air masses are parameterized. The model simulates the behavior of nitrogen oxides, nitric acid, water vapor, methane, hydrogen radicals, chlorine compounds, and ozone. It reproduces important features observed during different Antarctic and Arctic observation campaigns. The ozone hole in the southern hemisphere can only be simulated when the heterogeneous polar chemistry is taken into account. The springtime ozone depletion over Antarctica calculated in the model is thus mostly the result of chemical removal although the dynamics is responsible for the low temperature that triggers the large ozone loss rates. Unresolved questions are related to the strength of the vertical exchanges inside the vortex, the preconditioning of trace gases before and during the winter season, the behavior of the different trace gases as the vortex breaks down (dilution effects), accurate determination of the ozone sink inside the vortex, and a better quantitative estimation of the role of polar stratospheric clouds. Despite elevated concentrations of active chlorine at high latitudes in the northern hemisphere in late winter, no ozone hole is produced by the model, even with chlorine levels as high as 6 ppbv. This conclusion could, however, be modified for very stable and cold winters with delayed final warming.

1. Introduction

The discovery by *Farman et al.* [1985] of a substantial reduction in the October mean ozone column over Halley Bay, Antarctica, since the mid-1970s and the subsequent finding [*Stolarski et al.*, 1986] that this springtime "ozone hole" covers an area as large as the entire Antarctic continent came as a surprise to the scientific community involved in stratospheric research. Indeed, no chemical mechanism known at that time could account for the observed ozone destruction during September and no obvious change in the circulation patterns had been reported during the late 1970s or the early 1980s. No model had predicted the rapid decrease of the ozone concentration detected between 10 and 22 km altitude [*Hofmann et al.*, 1987]. Observations made since 1986 by ground-based instruments during two National Ozone Expeditions (NOZE) at the McMurdo station (Antarctica) and by airborne instruments during the Airborne Antarctic Ozone Experiment (AAOE) campaign gave clear evidence that the chlorine chemistry is significantly perturbed inside the Antarctic polar vortex in spring, i.e., that the level of active chlorine in the lower stratosphere is 50 to 100 times higher than at mid-latitudes. In particular, measurements made from an ER-2 aircraft flying at 18.5 km [*Anderson et al.*, 1988, 1989*a*, *b*] showed that the mixing ratio of ClO could reach slightly more than 1 ppbv and that, by the end of September, the densities of ozone and chlorine monoxide were highly anticorrelated on essentially all resolvable scales, suggesting a strong effect of chlorine on polar ozone in spring. Evidence was also found in the laboratory [*Molina et al.*, 1987; *Tolbert et al.*, 1987; *Leu*, 1988] that active chlorine is produced by heterogeneous processes on the surface of frozen particles such as those found in polar stratospheric clouds (PSCs). *Solomon et al.* [1986] had suggested earlier that active chlorine was probably released from the ice-catalyzed reaction of hydrogen chloride (HCl) with chlorine nitrate ($ClONO_2$).

Essentially two types of stratospheric clouds are observed in the cold air masses over Antarctica [*McCormick and Trepte*, 1986, 1987; *Poole and McCormick*, 1988; *Turco et al.*, 1989]. Type I PSCs are formed at temperatures lower than approximatively 195 K near 15–20 km altitude and are believed to be composed of nitric acid trihydrates ($HNO_3 \cdot 3H_2O$). The size of the particles is of the order of 1 μm, so that limited sedimentation takes place in this case. Type II PSCs are mostly composed of water ice, and can exist for temperatures lower than approximately 187 K in the lower stratosphere. The size of these particles is of the order of 10–100 μm, so that they are expected to fall at a rate of several kilometers per week [*Turco et al.*, 1989]. Probably as a result of the sedimentation of these particles, the Antarctic vortex becomes highly dehydrated [*Ramaswamy*, 1988; *Kelly et al.*, 1989] and denitrified [*Toon et al.*, 1986; *Fahey et al.*, 1989; *Gandrud et al.*, 1989] by the end of the winter, so that chlorine remains in the form of ClO, Cl_2O_2 and OClO rather than being locked into the $ClONO_2$ reservoir which would protect ozone from catalytical destruction by chlorine.

Satellite and other meteorological observations have provided information on the morphology and the evolution of the Antarctic vortex and its role as a containment vessel in which the perturbed chemistry takes place [*Stolarski et al.*, 1986; *Proffitt et al.*, 1988 ; *Krueger et al.*, 1988; *Hartmann et al.*, 1989].

[1]Permanent affiliation: Service d'Aéronomie, Centre National de la Recherche Scientifique, Paris, France.

Paper number 90JD01779.
0448-0227/91/90JD-01779$05.00

Although several uncertainties remain in many aspects of the perturbed chemistry in the polar regions as well as in the relative roles of dynamics and chemistry near the polar vortex, the gross features involved in the formation of the ozone hole are probably sufficiently well understood to be included as crude parameterizations in a multidimensional model of the middle atmosphere. The type of question that such a model can address deals, for example, with the different behavior of ozone and other trace gases in both hemispheres. The Arctic Airborne Stratosphere Experiment (AASE) that took place in January and February 1989 has shown [*United Nations Environmental Program/World Meteorological Organization* (UNEP/WMO), 1990] that the chlorine chemistry in the Arctic is also highly perturbed during winter in the vicinity of polar stratospheric clouds, but that ozone is much less significantly depleted than in Antarctica, (if depleted at all) since the breakup of the vortex takes place much earlier in the season, when the polar night is still present over these regions.

Theoretical studies of the perturbed polar chemistry have been based mostly on zero- or one-dimensional models [*Rodriguez et al.*, 1986; *Salawitch et al.*, 1988; *Douglass and Stolarski*, 1989; *Brühl and Crutzen*, 1990; *Henderson et al.*, 1990]. These simplified approaches are justified by the quasi-isolation of the polar vortex. A few studies have focussed on the dilution of the ozone-depleted air after the final warming, based on high resolution three-dimensional models [*Prather et al.*, 1990; *Cariolle et al.*, 1990] or on two-dimensional models [*Sze et al.*, 1989]. No explicit chemistry has been introduced in these three-dimensional (3D) models; rather, the ozone destruction rate has been parameterized by a loss specified in the polar vortex with a given time constant. Finally, Lagrangian photochemical studies [*Jones et al.*, 1989; *Austin et al.*, 1989] including a detailed treatment of airflow along isentropic trajectories have allowed the authors of these studies to calculate the photochemical ozone destruction, taking into account the effects of zonal asymmetries.

In the present paper, we use the mechanistic three-dimensional model described earlier by *Rose and Brasseur* [1989] in which a parameterization of the heterogeneous chemical processes taking place in the polar regions is included. This model and the initial conditions used for the integration are briefly described in section 2. In section 3, we present and discuss a simulation of the winter and spring evolution of trace gases (including ozone) in the lower stratosphere of the southern hemisphere. A model simulation for the northern hemisphere, also considered in section 3, should contribute to the interpretation of the observations made during the Arctic AASE expedition. A discussion and conclusions are presented in section 4. The resolution of the model used in this study is rather coarse in longitude, so that the details of the mixing processes associated with the breaking of the vortex after the final warming cannot be explicitly described. The model, however, captures most of the processes observed before the final warming and is therefore useful for studying the interaction of chemistry and dynamics during the formation phase of the ozone hole.

2. Model Description

The 3D mechanistic model used for this study is detailed by *Rose* [1983] and by *Rose and Brasseur* [1989]. It is hemispheric and extends from 8.5 to 80 km altitude, with 24 altitude pressure levels.

Dynamics

The 3D fields of wind components, temperature and geopotential heights are derived by solving the primitive equations on a 3D grid, with a resolution of 22.5° in longitude (wave number 4), 5° in latitude and 3 km in the vertical. A tropospheric forcing is applied at the lower boundary of the model (300 mbar) through a perturbed geopotential with the maximum amplitude and the phase of waves 1 to 3 chosen consistently with the climatological data reported by *Randel* [1987, 1988]. The latitudinal dependence of the amplitude of the forcing is expressed as in *Rose and Brasseur* [1989]. The amplitudes of each wave, adopted in the model, are assumed to remain constant over the entire integration period. In the southern hemisphere, where transient waves dominate, the maximum wave amplitudes adopted for the calculations are 100 geopotential meters (gpm), 120 gpm, and 120 gpm for waves 1, 2, and 3, respectively, with corresponding zonal phase velocities of 6, 11, and 14 degrees per day [*Randel*, 1988]. In the northern hemisphere, where large-scale standing waves dominate, wave number 3 forcing is ignored and the maximum amplitudes specified for wave numbers 1 and 2 are equal to 120 and 95 gpm, respectively. The zonal phase velocities are set equal to zero.

Rather than using a detailed radiative code, which would require large amounts of computer time, the net diabatic heating rate Q is parameterized as a function of temperature, T, by a Newtonian cooling approximation [*Dickinson*, 1973]:

$$\frac{Q}{C_P}=\alpha(z)[T-T_O(\phi,t,z)]$$

where $T_O(\varphi,t,z)$ is the climatological seasonally varying temperature toward which the model relaxes, and $\alpha(z)$ the Newtonian coefficient [see *Rose and Brasseur*, 1989]. This formulation implicitly introduces a seasonal forcing in the diabatic driving, but does not account for radiative feedbacks due to changes in the ozone concentration. *Kiehl et al.* [1988] have shown, based on the NCAR Community Climate Model, that an ozone hole (ozone depletion from 320 to 160 Dobson units (DU)) could cause coolings in the vortex of about 6 K by the end of October. Therefore, our model probably overestimates the temperature in the polar vortex when ozone is substantially depleted.

Chemistry

The density of 20 chemical species is calculated with a time step of 7.5 min. The short-lived species are grouped into three long-lived families $O_x = O_3 + O(^3P) + O(^1D)$, $NO_x = NO + NO_2 + NO_3 + HO_2NO_2$ and $ClO_x = Cl + ClO + 2\,Cl_2 + 2\,Cl_2O_2 + OClO + ClONO_2 + ClNO_2 + HOCl$. These families are transported as a whole and the mixing ratio of each individual species density is further calculated by assuming photochemical equilibrium between the different members of the families.

The nitrogen reservoirs N_2O_5 and HNO_3 are treated individually. The relatively slow conversion of NO_2 into N_2O_5 during nighttime, and the daytime photolysis of N_2O_5 into NO_2 are, therefore, explicitly simulated. The ClO_x family does not include HCl, which is treated as an individual species, as well as H_2O and CH_4. The fast-reacting hydrogenated radicals H, OH and HO_2 are assumed to be in photochemical equilibrium conditions. Note that, in this paper, Cl_x refers to $ClO_x + HCl$ and NO_y to $NO_x + HNO_3 + 2\,N_2O_5$.

The reaction rates in the gas phase are taken from *DeMore et al.* [1987]. The photodissociation rates are calculated from the solar irradiances compiled by *Brasseur and Simon* [1981] and from the absorption cross-sections given by *DeMore et al.* [1987]. In order to reduce the computer time required to integrate the equations, the diurnal variation of the photodissociation coefficients is expressed by assuming that the photolysis rate is equal to its mean daytime value in the sunlit atmosphere and is equal to zero during nighttime.

Parameterization of Polar Chemistry

Polar stratospheric clouds are known to initiate the perturbed chemistry observed in the polar regions. In the model, the formation of type I PSCs below 25 km altitude is assumed to occur instantaneously as soon as the temperature decreases below 199 K. The same applies to type II PSCs, but in this case the temperature threshold is chosen to be 194 K. These temperature thresholds are a few degrees higher than the actual thermodynamic values. This choice, however, is made to account for the fact that the temperatures, used in the model as initial and relaxation temperatures, are climatological values which do not reproduce the observed coldest airmasses, whose locations are highly variable in time and from year to year, especially in the northern hemisphere. Thus, rather than representing the specific thermodynamic conditions under which clouds are produced by microphysical processes, these thresholds define the atmospheric regions in which, statistically, clouds are assumed to be present.

The conversion of chlorine reservoirs to more reactive forms is assumed to occur on the surface of both types of PSCs particles through the following reactions [*Solomon et al.*, 1986]

$$ClONO_2(g) + HCl(s) \rightarrow Cl_2(g) + HNO_3(s) \quad (1a)$$

$$ClONO_2(g) + H_2O(s) \rightarrow HOCl(g) + HNO_3(s) \quad (1b)$$

$$N_2O_5(g) + HCl(s) \rightarrow ClNO_2(g) + HNO_3(s) \quad (1c)$$

$$N_2O_5(g) + H_2O(s) \rightarrow 2HNO_3(s) \quad (1d)$$

where g corresponds to the gas phase, and s to a solid or ice solution. The overall conversion time of nitrogen oxides (N_2O_5) to nitric acid is assumed to be 10 days (2 to 20 days according to *Toon et al.* [1989]). The chlorine molecules (Cl_2, HOCl, $ClNO_2$) released in the gas phase by these reactions do not directly affect ozone but, as soon as the Sun returns over Antarctica, are photolyzed and substantial amounts of reactive chlorine (Cl, ClO) are produced. The conversion of HCl to ClO_x is assumed to take place almost instantaneously. In the region where the temperature is below the threshold for the formation of type II PSCs, nitric acid produced by (1a)-(1d) is supposed to remain in the condensed phase and to be removed from the atmosphere (denitrification) by sedimentation at a rate of several kilometers per week [*Turco et al.*, 1989]. In the model, dehydration and denitrification, in the presence of type II particles, occur with a time constant of 5 days. The precise choice of this value does not affect the calculated ozone depletion which takes place in early spring, more than 2 months after these processes have begun to occur. This time constant is consistent with the conversion time of reactions (1a)-(1d) and the rate of sedimentation observed in the polar stratosphere (about 2 km week^{-1} for a 4 μm particle [see *McCormick et al.*, 1989]).

In the regions where the temperature is such that type I PSCs are formed, no dehydration takes place and denitrification should be modest, since the sedimentation velocity of these particles (typical radius of 1 μm) is substantially lower than that of larger ice particles in type II PSCs. During the AASE campaign, very little evidence for denitrification was found prior to late January 1989, but extensive denitrification was observed near 20 km in early February [*UNEP/WMO*, 1990]. Observed column abundances of nitric acid were substantially higher than in Antarctica (W. G. Mankin and M. T. Coffey, private communication, 1989), but in situ measurements of NO_y near 12 km suggested enhancements of the local NO_y concentration, possibly through evaporation of particles sedimented from higher levels [*UNEP/WMO*, 1990]. The mechanisms involved are still poorly understood and, therefore, two extreme cases have been considered. In the first of them (case 1S or N), denitrification with a characteristic time constant of 15 days has been assumed in the regions where PSCs I are present. In the other case (case 2S or N) no denitrification has been considered in these regions. Such sensitivity study put constraints, especially in the Arctic regions, where most of the perturbed chemistry appears to be associated with the presence of type I PSCs. Unless otherwise specified, the results presented hereafter will refer to cases with denitrification (cases 1N and 1S) in regions where type I PSCs are formed.

Finally, the model assumes that, besides the classic catalytical cycles which contribute to the ozone budget in the background atmosphere [e.g., *Solomon et al.*, 1986; *Brasseur and Solomon*, 1986], ozone is destroyed in the chemically perturbed regions by the following cycles involving the formation of the ClO dimer [*Molina and Molina*, 1987; *Molina et al.*, 1987]

$$2(Cl + O_3 \rightarrow ClO + O_2) \quad (2a)$$

$$ClO + ClO + M \rightarrow Cl_2O_2 + M \quad (2b)$$

$$Cl_2O_2 + h\nu \rightarrow Cl + ClOO \quad (2c)$$

$$ClOO + M \rightarrow Cl + O_2 + M \quad (2d)$$

$$\text{Net: } 2O_3 \rightarrow 3O_2$$

and

$$2(Cl + O_3 \rightarrow ClO + O_2) \quad (3a)$$

$$ClO + ClO + M \rightarrow Cl_2O_2 + M \quad (3b)$$

$$Cl_2O_2 + M \rightarrow Cl_2 + O_2 + M \quad (3c)$$

$$Cl_2 + h\nu \rightarrow 2Cl \quad (3d)$$

$$\text{Net: } 2O_3 \rightarrow 3O_2$$

and by an additional cycle requiring the presence of bromine [*McElroy et al.*, 1986]

$$Cl + O_3 \rightarrow ClO + O_2 \quad (4a)$$

$$Br + O_3 \rightarrow BrO + O_2 \quad (4b)$$

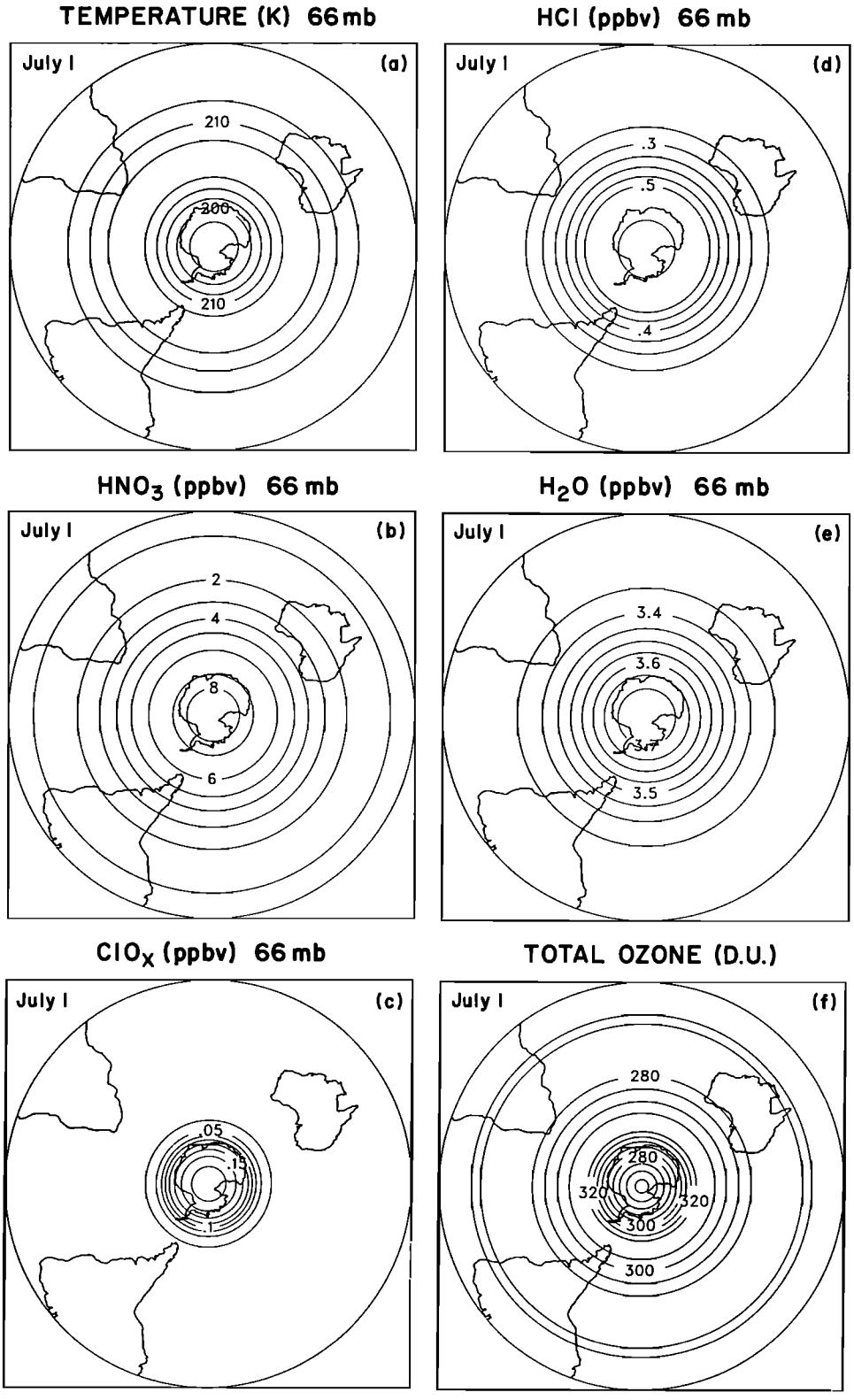

Fig. 1. Initial conditions for the model on the 66 mbar isobaric level: (*a*) temperature (K) on July 1 in the southern hemisphere; (*b*) HNO_3 (ppbv); (*c*) ClO_x (ppbv) (inorganic chlorine without HCl); (*d*) HCl (ppbv); (*e*) H_2O (ppmv); and (*f*) total ozone column (Dobson units) on July 1 in the southern hemisphere and on January 1 in the northern hemisphere. Contour intervals: (*a*) 5 K, (*b*) 1 ppbv, (*c*) 25 pptv, (*d*) 0.05 ppbv, (*e*) 0.25 ppbv, and (*f*) 10 DU.

$$BrO + ClO \rightarrow Br + Cl + O_2$$

$$\text{Net: } 2O_3 \rightarrow 3O_2$$

Note that the BrO + ClO reaction is characterized by an other channel leading to the formation of OClO.

The rate limiting steps for cycles 2, 3, and 4 are assumed to be reactions (2*b*), (3*b*), and (4*c*), respectively, whose rates as a function of temperature and reaction products have been measured only recently. For reactions (2*b*) and (3*b*), we are using the rate constant measured by *Sander et al.* [1989]. For reaction (4*c*), the rate constant recommended of *DeMore et al.* [1987] is used. Since the chemistry of bromine is not explicitly treated in the model, a constant mixing ratio of 10 pptv is chosen for BrO, consistently with observational data [e.g., *Solomon et al.*, 1989].

Initial Conditions

Model simulations have been performed for both hemispheres, with the purpose of studying the behavior of ozone in winter and spring over the two polar regions. The simulations start on July 1 and January 1 for the southern and northern hemispheres, respectively. Since no waves are initially present, the model integration starts with zonally symmetric fields of dynamical and chemical variables. The mean climatological zonal winds compiled by *Randel* [1987] are used as initial values. The initial temperature field is derived, assuming a gradient wind balance with geopotential heights.

The initial distributions of the chemical species are taken from the two-dimensional model of *Brasseur et al.* [1990]. Figure 1*a* presents the (July 1) distributions of temperature in the southern hemisphere at 66 mbar, while Figures 1*b*-1*e* show the initial distributions of HNO_3, ClO_x, HCl, and H_2O specified initially in both hemispheres at the same isobaric level. The initial value of total ozone is shown in Figure 1*f*. As seen in Figure 1*a*, the southern hemisphere temperature is lower than 200 K above the pole. For the simulations of present-day conditions (cases 1 and 2), the mixing ratio of inorganic chlorine ($Cl_x = ClO_x + HCl$) near 30 km altitude is 2.8 ppbv (corresponding approximately to mid-1980s conditions [see *UNEP/WMO*, 1990]), and, at 66 mbar (18 km) the maximum initial mixing ratio of ClO_x (inorganic chlorine without HCl) over the pole is 0.25 ppbv.

3. Model Simulations

In order to investigate the behavior of the polar atmosphere under various conditions, different model simulations have been performed (see Table 1). This analysis will focus on results obtained in the lower stratosphere, where the chemistry is perturbed by the presence of PSCs; most results for the southern hemisphere will be shown on the 66 mbar isobaric surface (approximately 18 km). Since, near the North Pole, the coldest temperatures are found at somewhat higher altitudes, (4*c*) most results obtained for northern hemisphere simulations will be shown on the 43 mbar (21 km) level.

TABLE 1. Model simulations

Case No. *	Inorganic chlorine Level (ppbv)	Denitrification by Type I PSCs
1 S and N	2.8	yes
2 S and N	2.8	no
3 S	1.4	yes
4 S and N	6.0	yes

*S and N refer to the southern and northern hemispheres, respectively.

The Southern Hemisphere

The first of these model runs (case 1S) is intended to reproduce the dynamics and chemistry of the southern hemisphere for levels of odd chlorine corresponding to the mid 1980s. The model is initiated on July 1 by zonally symmetric temperature and trace gas fields and is forced by transient waves, as specified in section 2. Figures 2*a*-2*b* show the dynamical fields calculated for August 15. A strong nearly

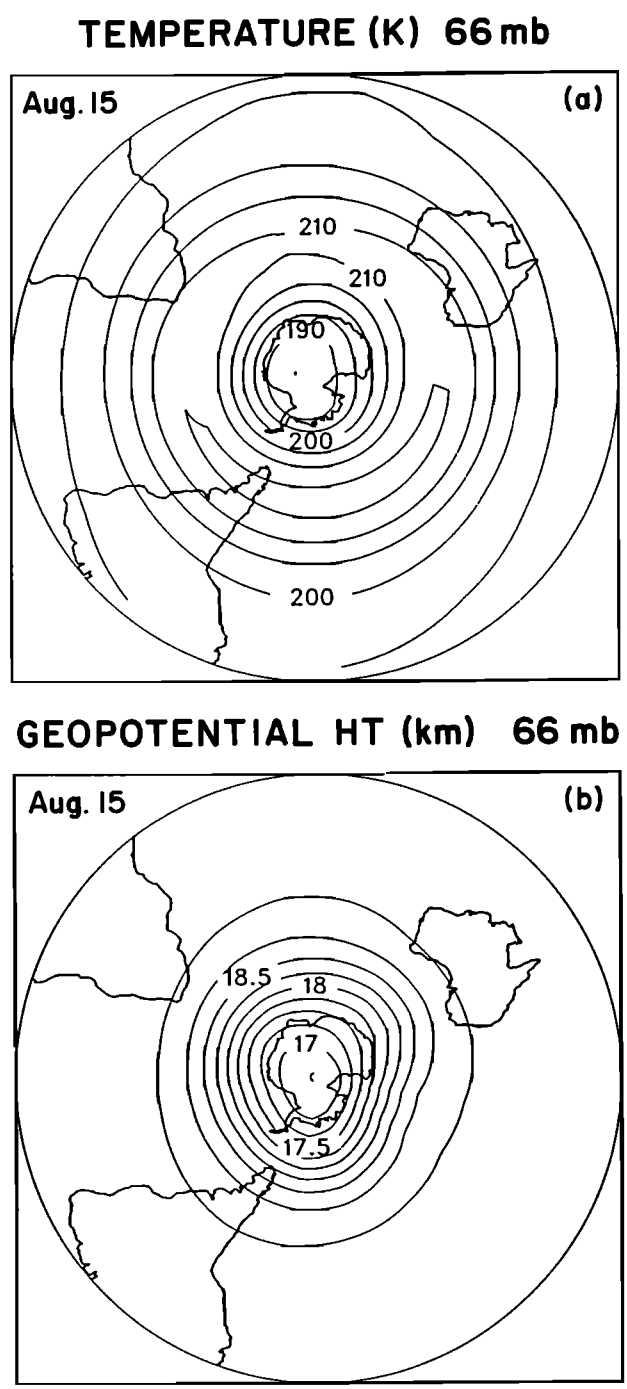

Fig. 2. Temperature (K) and geopotential height (km) on the 66 mbar surface in the southern hemisphere on August 15. Contour intervals: (*a*) 5 K and (*b*) 0.25 km.

symmetric vortex is located over the polar region with the geopotential height decreasing from 19.25 km at 60°S to 17 km over the pole. The temperature distribution is also nearly axi-symmetric although the maximum, found at the edge of the vortex (215–220 K), exhibits a "croissant" shape in agreement with the observations [e.g., *Shiotani and Gille,* 1987]. The temperature over the pole reaches a minimum of less than 190 K. Polar clouds are thus present over the Antarctic during this period, and chemical processes associated with the presence of these clouds are occurring. Figure 3*a* shows that, already in August, the polar lower stratosphere is dehydrated. The mixing ratio of H_2O decreases to about 1 ppmv, compared with values of about 3.5 ppmv immediately outside the dehydration edge. This type of behavior simulated by the model is consistent with observations [*Kelly et al.,* 1989], although the calculated water vapor mixing ratio inside the vortex is somewhat smaller than the value observed during the AAOE campaign (1.5 ppmv). In the case of odd nitrogen (Figures 3*b*-3*d*), NO_x(~NO+NO_2) in the polar night is transformed into N_2O_5 as a result of the reaction between NO_2 and ozone and, through heterogeneous processes, (1*c*)and (1*d*), on the surface of ice particles in PSCs I and II, N_2O_5 is converted into nitric acid. Since the temperature over the pole is lower than the specified threshold under which type II PSCs are present, HNO_3 is rapidly removed from the stratosphere through sedimentation of the PSC particles. The polar atmosphere is denitrified. At the same time, a large fraction of HCl is converted in more active forms of chlorine compounds (ClO_x). In the polar night, the chlorine released from heterogeneous reactions (1*a*)-(1*c*) is in the form of Cl_2, HOCl, or $ClNO_2$ and does not affect ozone. As shown in Figures 4*a*-4*b*, the concentration of HCl over the polar region is significantly depleted and that of ClO_x substantially elevated (about 800 pptv). Very small concentrations of ClO however are present at this time of the year. The distribution of the ozone column calculated for August 15 (Figure 5) results therefore primarily from transport processes in the lower stratosphere, which produces the croissant type maximum (about 340 DU) in the warm belt near 60° latitude and the minimum of about 250 DU inside the polar vortex. Thus, contrary to what is observed in the northern hemisphere, where the maximum of the ozone column abundance is located at the North Pole in late winter, the ozone column exhibits a small minimum over the South Pole during this season. This type of behavior was already noted by *Dobson* [1956] and is now well documented [e.g., *London,* 1980]. The values at the South Pole in August are, however,

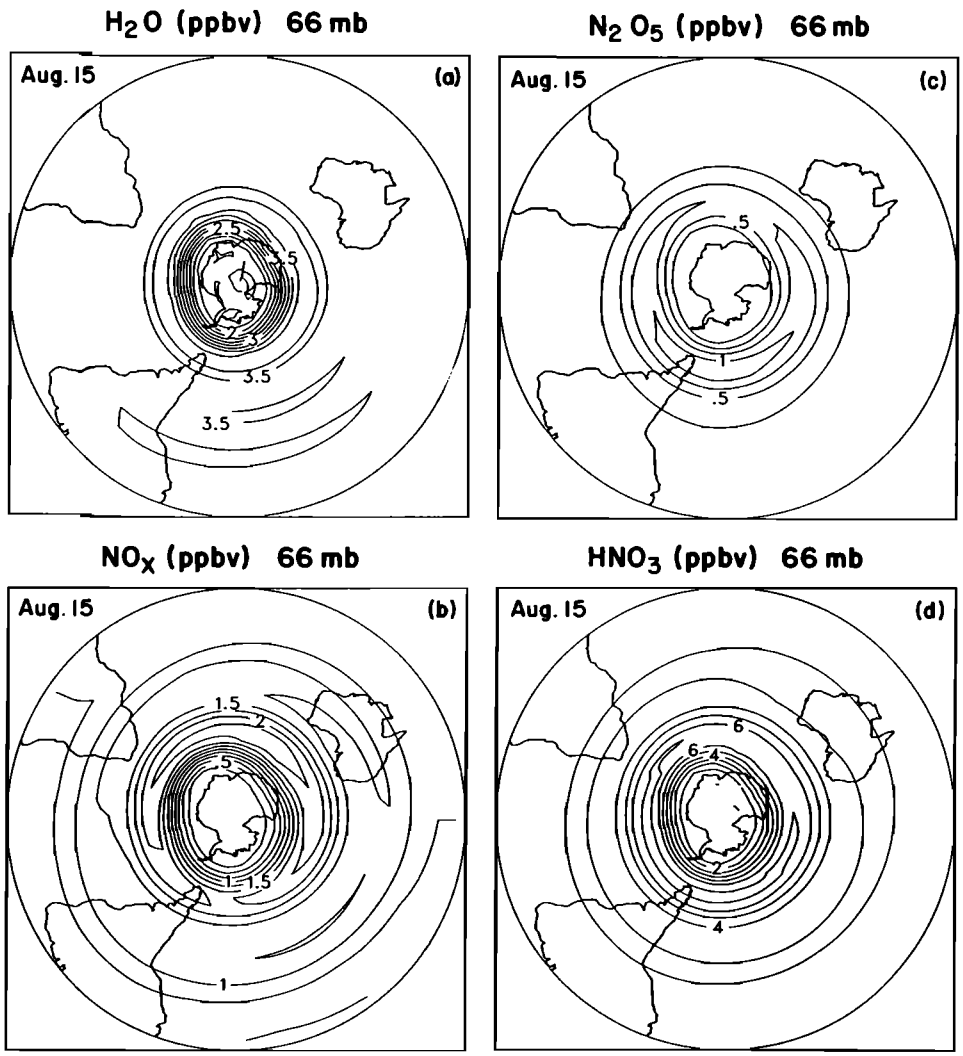

Fig. 3. Distribution on the 66 mbar surface of (*a*) water vapor (ppmv); (*b*) NO_x (ppbv); (*c*) N_2O_5 (ppbv); (*d*) HNO_3 (ppbv) mixing ratios in the southern hemisphere on August 15 (case 1S). Contour intervals: (*a*-*c*) 0.25 ppbv and (*d*) 1 ppbv.

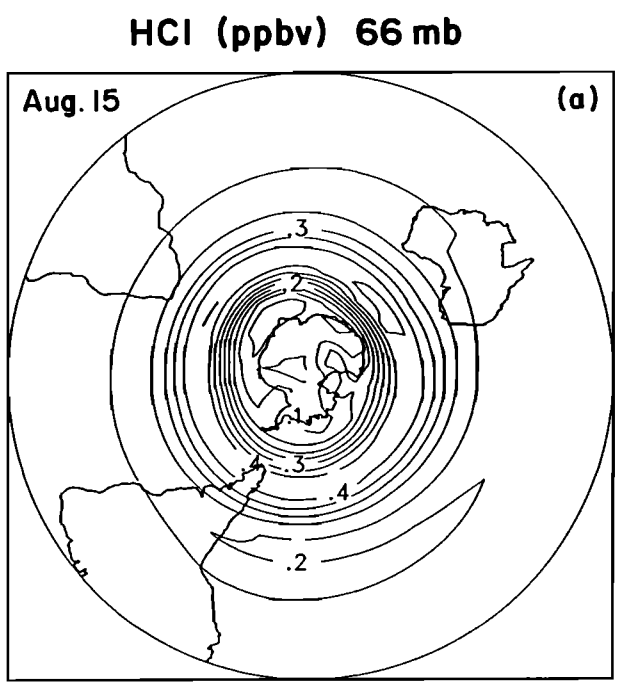

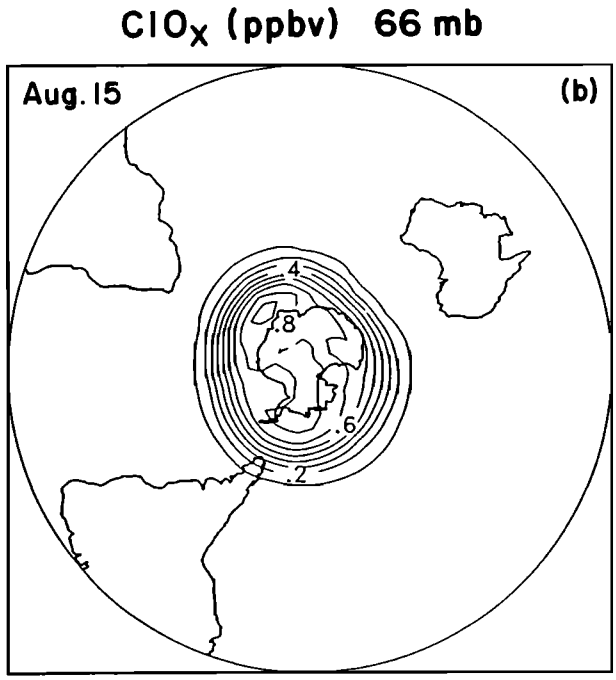

Fig. 4. Distribution on the 66 mbar surface of (*a*) HCl (ppbv) and (*b*) ClO_x (ppbv) mixing ratio in the southern hemisphere on August 15 (case 1S). Contour intervals: (*a*) 0.05 ppbv and (*b*) 0.1 ppbv.

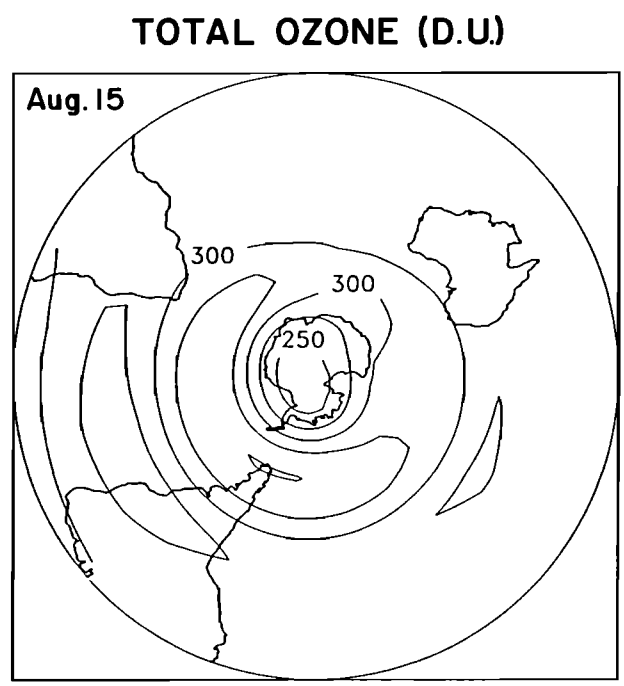

Fig. 5. Distribution of the ozone column abundance (Dobson units) in the southern hemisphere on August 15 (case 1S). Contour interval: 25 DU.

substantially larger than the values observed in September and October since the late 1970s.

The fields calculated by the model (case 1S) in October will now be described. At this time of the year, the Sun has returned to the Antarctic region and the catalytic cycles believed to destroy ozone are operating. The dynamical fields produced by the model are quantitatively similar to those produced during August: the vortex is centered over the pole; the temperature is lower than 197 K in the vortex and reaches a maximum of about 220 K near 60° latitude. The morphology of water vapor, nitrogen oxides, and nitric acid (not shown) has not significantly changed, although the area of the polar region affected by dehydration and denitrification has slightly increased. The mixing ratio of ClO_x in the chemically perturbed region reaches 800 pptv (Figure 6*a*) and, in the polar region where solar radiation penetrates (daytime), ClO is produced (Figure 6*b*): its calculated mixing ratio reaches nearly 600 pptv. In the polar region during nighttime, ClO reacts with itself to produce the Cl_2O_2 dimer; very little ozone destruction takes place. It is interesting to examine how the individual oxides of nitrogen NO and NO_2 behave. Figures 7*a*-7*b* show that, on the 66 mbar isobaric surface, the mixing ratios of NO and NO_2 at mid- and low latitudes are very similar during daytime (about 0.5 ppbv) and that NO is almost entirely converted into NO_2 during nighttime. The conversion of NO_2 to N_2O_5 during nighttime and photodecomposition of N_2O_5 to NO_2 during daytime explains the weak component of the diurnal variation affecting the distribution of the nitrogen oxides ($NO + NO_2$). Finally, the large latitudinal gradients seen in the mixing ratio of these species at the edge of the polar vortex is associated with the denitrification occuring over the Antarctic continent. A sharp meridional gradient in the NO_2 mixing ratio, especially during nighttime is visible at high latitude. The location of this discontinuity is moved towards the pole, when denitrification in type I PSCs is omitted (case 2S, not shown). In this case, the ClO produced by heterogeneous processes is converted into chlorine nitrate: a strong maximum in the $ClONO_2$ concentration is then found in the region of PSCs I.

The total ozone abundance calculated for October 3 is shown in Figure 8. As in August, the ozone column is largest in the warm belt near 60° latitude (400 DU) and smallest over the South Pole. But, this time, this minimum value (approximately 180 DU) is 80 DU lower than in mid-August. A minimum ozone

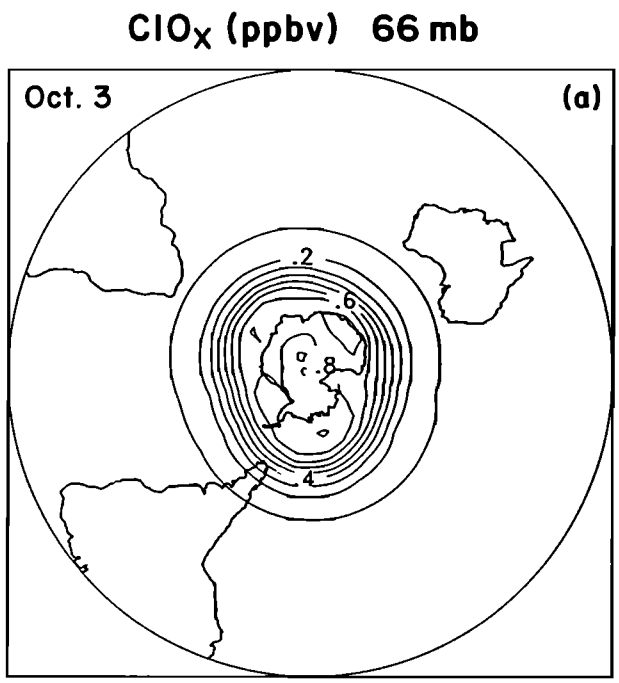

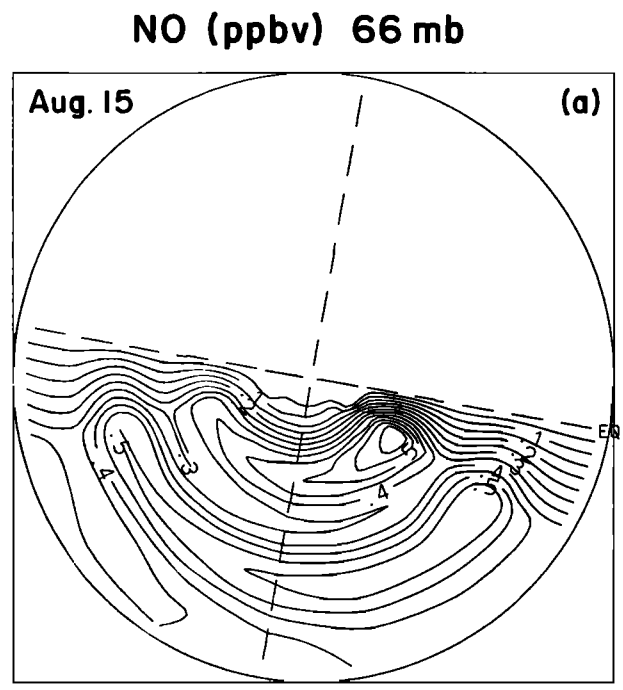

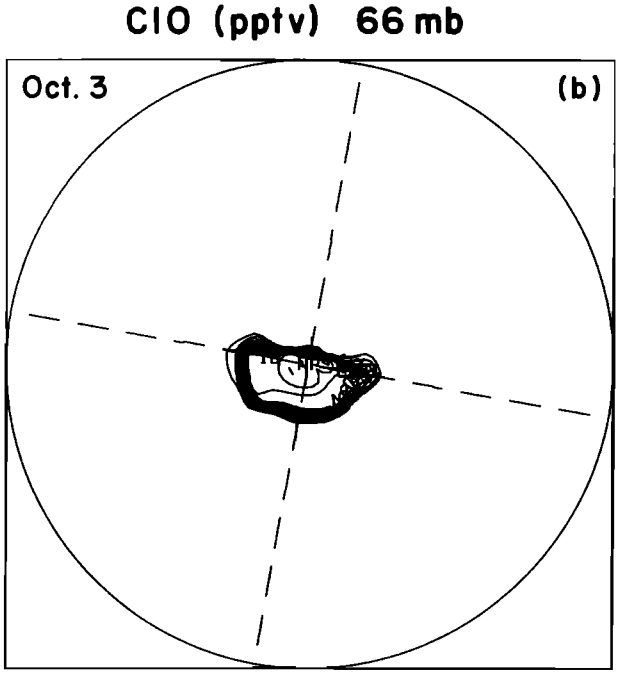

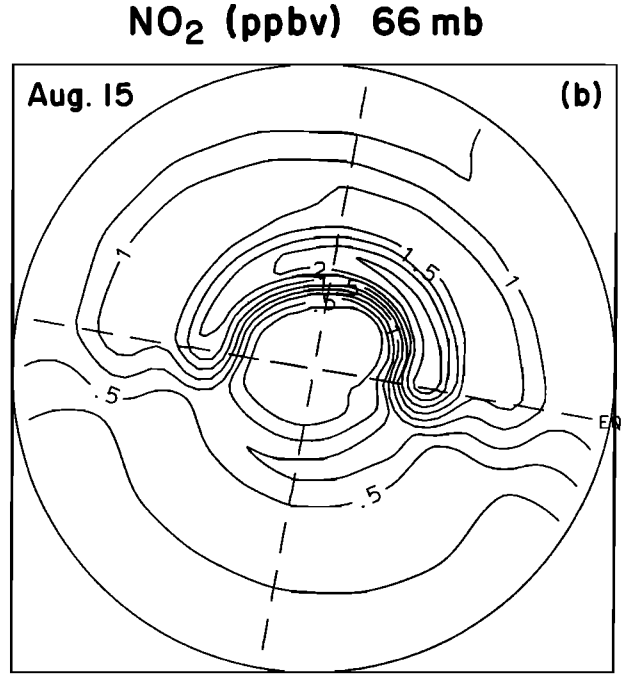

Fig. 6. Distribution on the 66 mbar surface of (*a*) ClO_x (ppbv), and (*b*) ClO (ppbv) mixing ratios in the southern hemisphere on October 3 (case 1S). Contour intervals: (*a*) 0.1 ppbv and (*b*) 100 pptv.

Fig. 7. Same as Figure 4 but for (*a*) NO (ppbv) and NO_2 (ppbv) mixing ratios (August 15). Contour intervals: (*a*) 0.05 ppbv and (*b*) 0.25 ppbv.

column of 158 DU is obtained on October 17. As will be shown later, this calculated decrease results from the rapid chemical destruction of ozone by active chlorine. As time proceeds, diabatic processes heat the polar atmosphere and, as the final warming appears, the polar vortex breaks up. In early November, as shown in Figures 9*a*-9*b*, the ozone-poor airmass is removed from the pole and is gradually replaced by a mass of ozone-rich air. At this time, the ozone maximum is as high as 500 DU. The resolution of the model, however, is too coarse to simulate the details of the planetary wave breaking, the cascade of energy to smaller scales and the related irreversible mixing of air during this period [see *Rose and Brasseur*, 1989].

In order to estimate the role of the chlorine chemistry in the formation of the ozone hole, a simulation has been performed for the same conditions but with an amount of inorganic chlorine (Cl_x) representative of the early 1970s (case 3S). The mixing ratio of Cl_x in this case is chosen to be equal to 1.4 ppbv rather than 2.8 ppbv as in the previous model run. The difference in the ozone column abundance calculated for these two chlorine levels are relatively small in August (not shown):

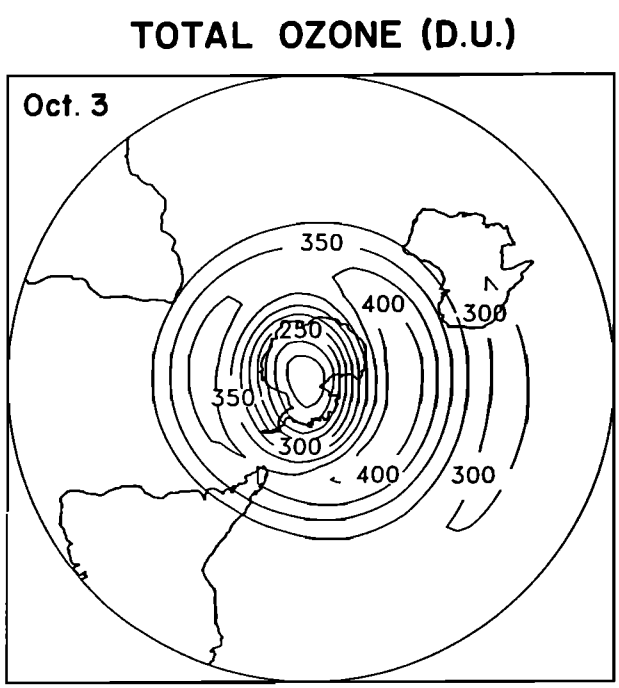

Fig. 8. Same as Figure 5 but for October 3. Contour interval: 25 DU.

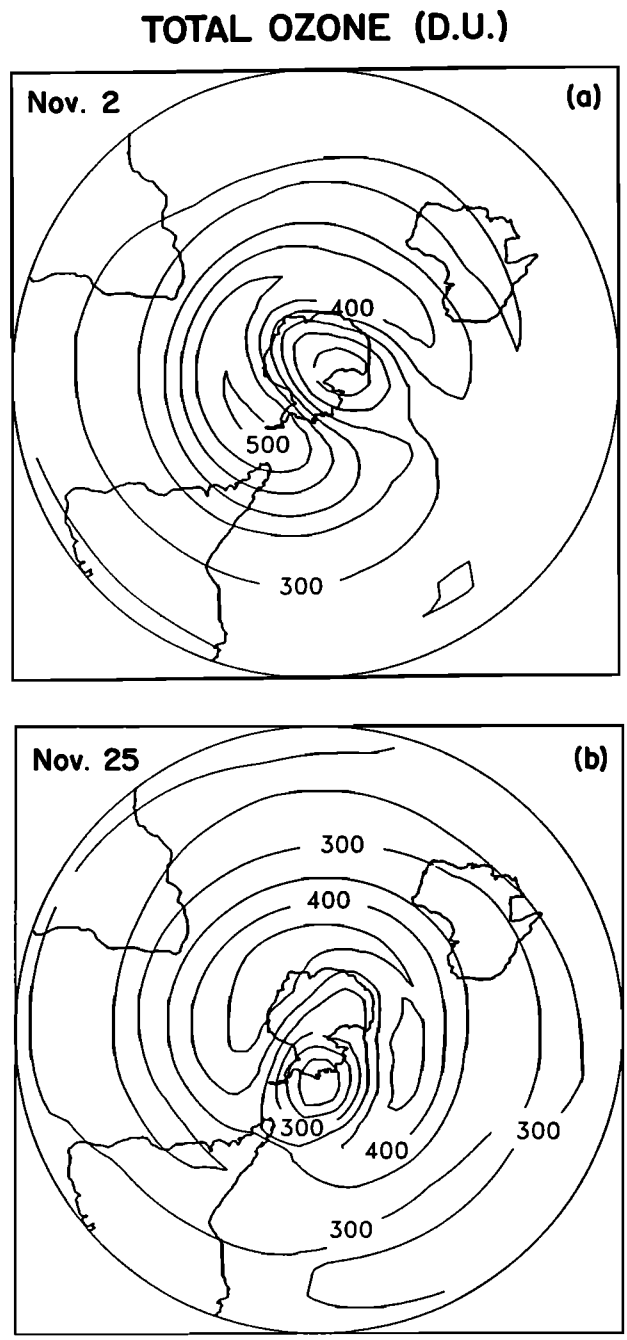

Fig. 9. Calculated ozone column abundance (Dobson units) in the southern hemisphere during November. Contour intervals: 50 DU.

about 1% at mid-latitudes, 3% at high latitudes near the terminator, and insignificant changes in the polar night region. In early October, the difference between the ozone column calculated for 1.4 ppbv and 2.8 ppbv, respectively is larger than 20% over the South Pole (Figure 10*a*). Clearly (Figure 10*b*), the ozone minimum, already present in August and associated with dynamical processes remains at the same level during September and October. In early October, the ozone column over the pole reaches 250 DU and is thus 70 DU higher than for levels of inorganic chlorine reaching 2.8 ppbv. The change in the ozone density near the South Pole takes place primarily in the 10–26 km altitude range. On October 15, the calculated reductions, when Cl_x increases from 1.4 to 2.8 ppbv, are 75% at 10 km, 65% at 13 km, 45% at 16 km, 33% at 19 km, 23% at 22 km, 17% at 25 km, and 2% at 28 km. The change calculated at 10 km might be inaccurate, as it is strongly affected by the condition at the lower boundary of the model, which remains unchanged during the entire integration. The ozone hole simulated by the model is the primary result of a chemical effect.

Finally a model simulation (case 4S) is performed with enhanced chlorine amounts (6 ppbv). The purpose of this run is to estimate potential future changes in response to further emissions in the atmosphere of chlorofluorocarbons and other halocarbons. The difference in total ozone calculated for August 15 reaches about 15% near the terminator and is smaller than 2% at the pole due to the lack of solar radiation required for the catalytic cycle to destroy ozone. On October 3 (Figure 11*a*), the ozone column is lower than 100 DU and therefore significantly lower than for present levels of inorganic chlorine. At the South Pole on October 15, the calculated depletion, when the level of chlorine increases from 1.4 to 6 ppbv, is 75% at 19 km, 52% at 22 km, 28% at 25 km, and 5% at 28 km. Below 18 km, nearly all the ozone is destroyed. Again, this purely chemical effect does not take into account possible temperature feedbacks. This feedback mechanism could extend the region of low temperatures towards lower latitudes and expand the area of the ozone hole. The evolution, as a function of time, of the ozone column abundance derived at the South Pole for different levels of odd chlorine is shown in Figure 11*b*. With chlorine amounts of 6.0 ppbv, expected in the middle of the twenty-first century in the framework of the Montreal Protocol on the Protection of the Ozone Layer [*UNEP/WMO*, 1990], a value as low as 60 DU is predicted on October 15. This extremely low value is obtained since the depletion extends over an altitude range of approximately 12 to 24 km.

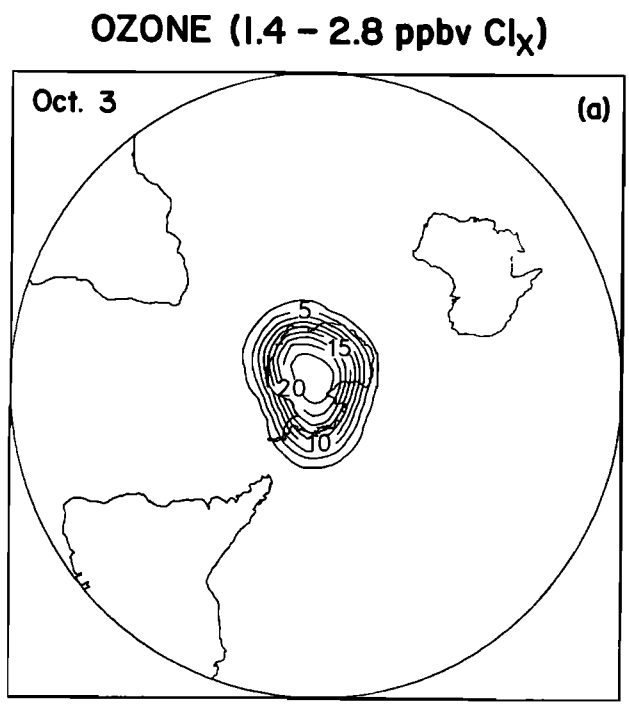

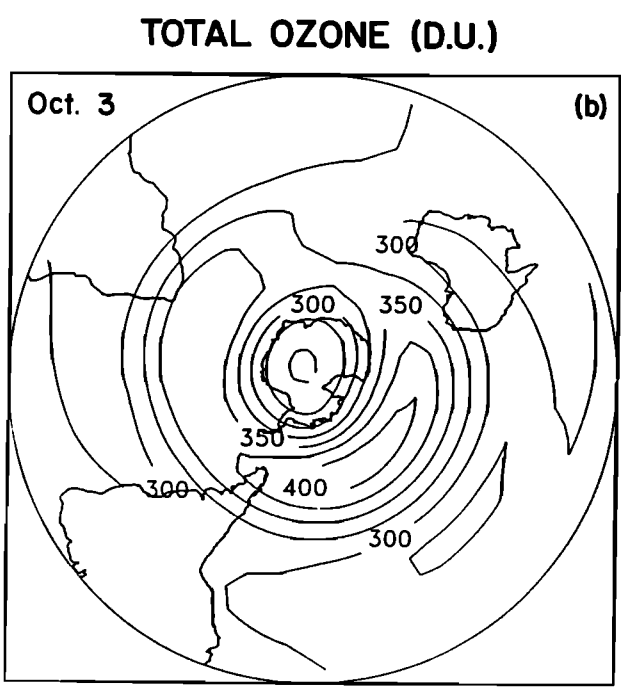

Fig. 10. (*a*) Depletion in the ozone column (percent) in the southern hemisphere (October 3) calculated for an increase in odd chlorine from 1.4 to 2.8 ppbv. (*b*) Ozone column abundance (Dobson units) in the southern hemisphere (October 3) calculated for a level of Cl_x (1.4 ppbv) representative of the early 1970s (case 3S). Contour intervals: (*a*) 5% and (*b*) 25 DU.

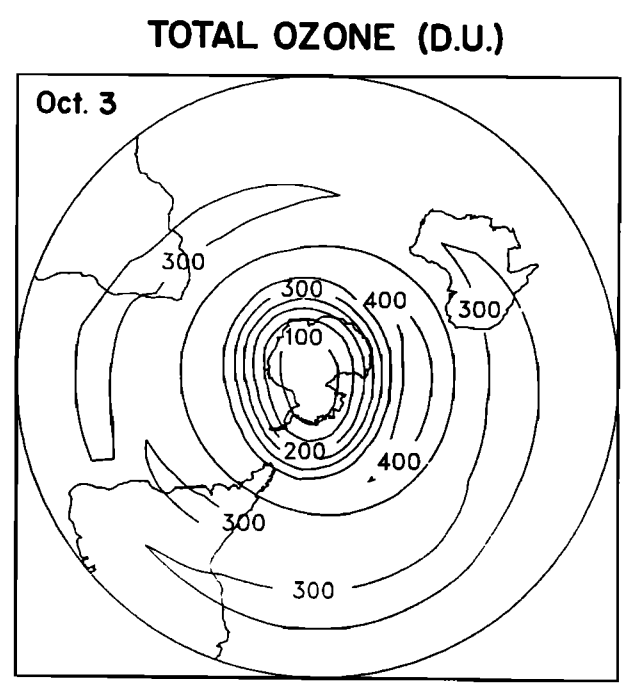

Fig. 11*a*. Ozone column abundance (Dobson units) in the southern hemisphere calculated for a level of odd chlorine equal to 6 ppbv (case 4S). Contour interval: 50 DU.

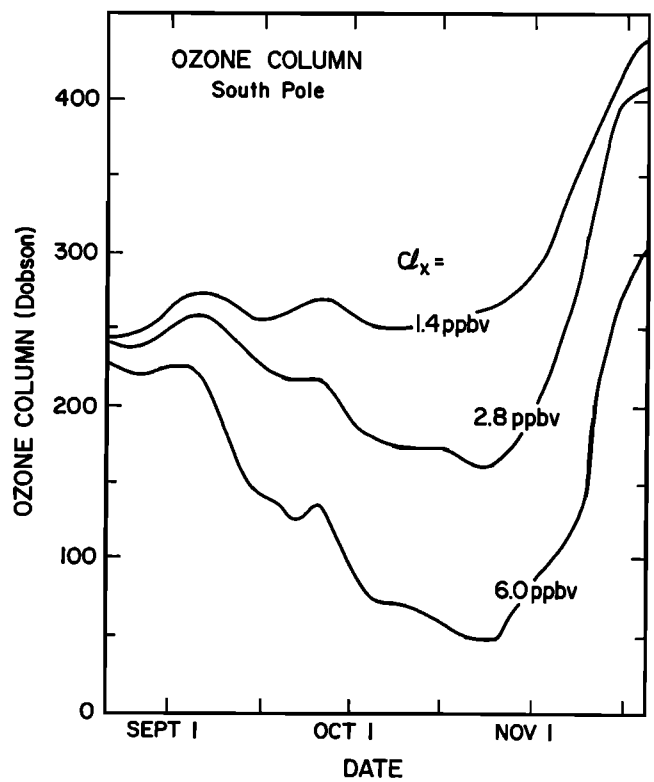

Fig. 11*b*. Ozone column abundance (Dobson units) as a function of time at the South Pole for three different levels of odd chlorine (Cl_x).

The Northern Hemisphere

As shown by climatological data, the coldest temperatures in the polar lower stratosphere of the northern hemisphere are found at a somewhat higher altitude than in the southern hemisphere. The model results concerning the Arctic regions will therefore be shown on the 43 mbar level (about 21 km) rather than at 66 mbar (about 18 km) as in the previous discussion. Due to the more pronounced topography in the northern hemisphere, the tropospheric forcing by planetary waves, especially wave number 1, is stronger than in the southern hemisphere and the calculated dynamical fields in the

entire stratosphere are significantly more disturbed than in the previous model simulations. Figures 12*b*-12*c* show, for example, the temperature fields on January 15 and February 14, respectively. In both cases, the wave structure is clearly visible. On January 15, for example, warm air is predicted to be present over Japan and the northern Pacific Ocean and cold air over northern Europe and northern Siberia. The coldest temperatures, found over northern Scandinavia, are close to 200 K, so that only type I PSCs will eventually be formed. On February 14, the warmest air is found over the North American continent and the coldest air over the pole.

During the winter season, as shown by Figure 13*a*, the concentration of NO_x ($NO + NO_2$) is very low in the region of the polar night because of the rapid reaction of NO_2 with ozone, producing NO_3, which in turn, is converted into N_2O_5 by a further reaction with NO_2. The inverse transformation of N_2O_5 to NO_2 and NO is very slow since no photolysis takes place in the polar night. The conversion of N_2O_5 to nitric acid takes place in the region where PSCs are present (Figure 13*b*–13*c*), but, since the model does not produce on the 43 mbar level the cold temperatures required for PSCs II to be formed, nitric acid is only slowly (case 1N) or even not (case 2N) removed from the atmosphere by sedimentation processes, depending on the assumption made for the denitrification rate. Figures 13*b*–13*d* (January 15) clearly show the region over northern Siberia in which heterogeneous conversion by PSCs I of N_2O_5 to HNO_3 takes place. They also indicate that, over this area, the mixing ratio of HNO_3 reaches 18 ppbv in the absence of denitrification (Figure 13*d*, case 2N) but only 13 ppbv when moderate denitrification is assumed to take place (Figure 13*c*, case 1N). At the end of the winter, in contrast to what is calculated and observed over Antarctica, a HNO_3 maximum covers the entire North Pole region in both cases. Thus, at this level, the model suggests that nitrogen oxides are transformed into nitric acid (a process sometimes referred to as denoxification) but that denitrification is less effective than in Antarctica. Similarly, contrary to what is derived and observed over the South Pole, the model does not produce any dehydration near the North Pole. It should be noted, however, that on the 28 mbar isobaric level where the temperature reaches values of less than 194 K at a few grid points of the model, small areas of dehydration are found during January. As mentioned earlier, it is important to note that particles, when transported downward, can evaporate as they encounter warmer layers and release in the gas phase the condensed nitric acid. Thus, on certain occasions, the sedimentation of these particles produces a net downward transport of gas phase nitric acid from cold to warmer regions of the atmosphere.

The presence of PSCs in the cold regions of the Arctic stratosphere leads to a rapid conversion of HCl into active ClO_x. As depicted in Figures 14*a*-14*b*, HCl on the 43 mbar level is substantially reduced and ClO_x substantially enhanced over northern Siberia, on January 15. The mixing ratio of ClO calculated at this time in this region is still small because of lack of solar radiation. A month later, on February 14, it is substantially higher but, because of limited denitrification, a fraction of ClO is reconverted into $ClONO_2$. The importance of this latter process depends on the degree of denitrification in the polar region and therefore on the geographical extent of the cold airmass region, which is influenced by the intensity of the planetary waves and therefore varies from year to year.

Despite values of active chlorine concentrations similar to that calculated in the southern hemisphere, the model does not

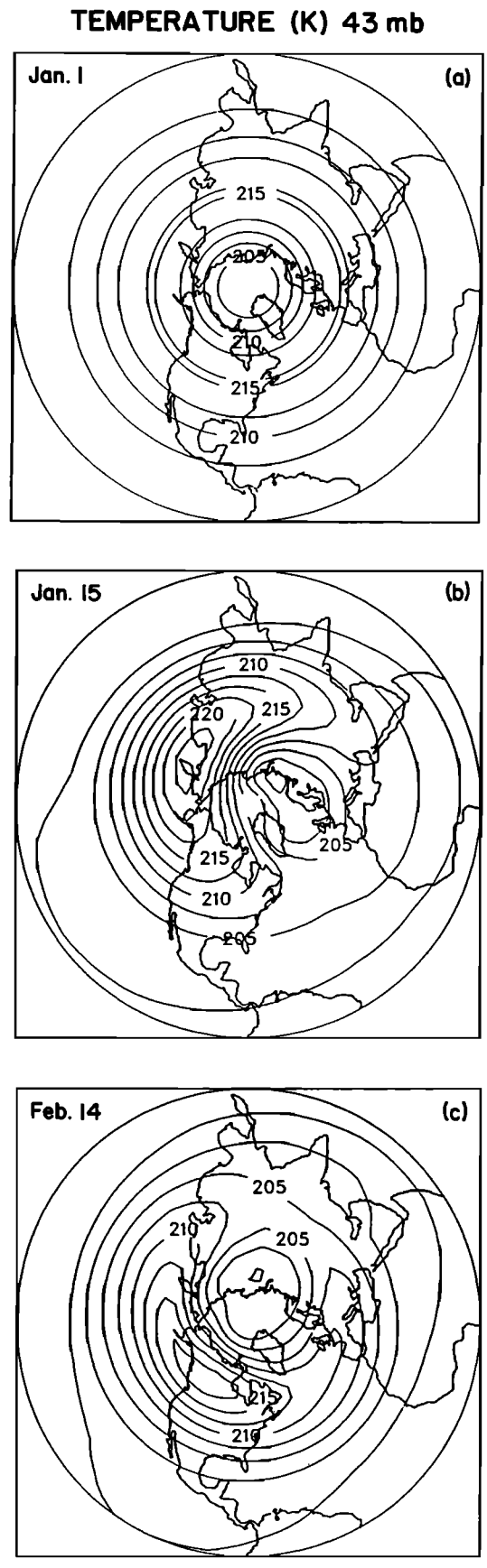

Fig. 12. Temperature (K) calculated in the northern hemisphere on the 43 mbar isobaric surface on (*a*) January 1 (initial value), (*b*) January 15, and (*c*) February 14. Contour interval: 2.5 K.

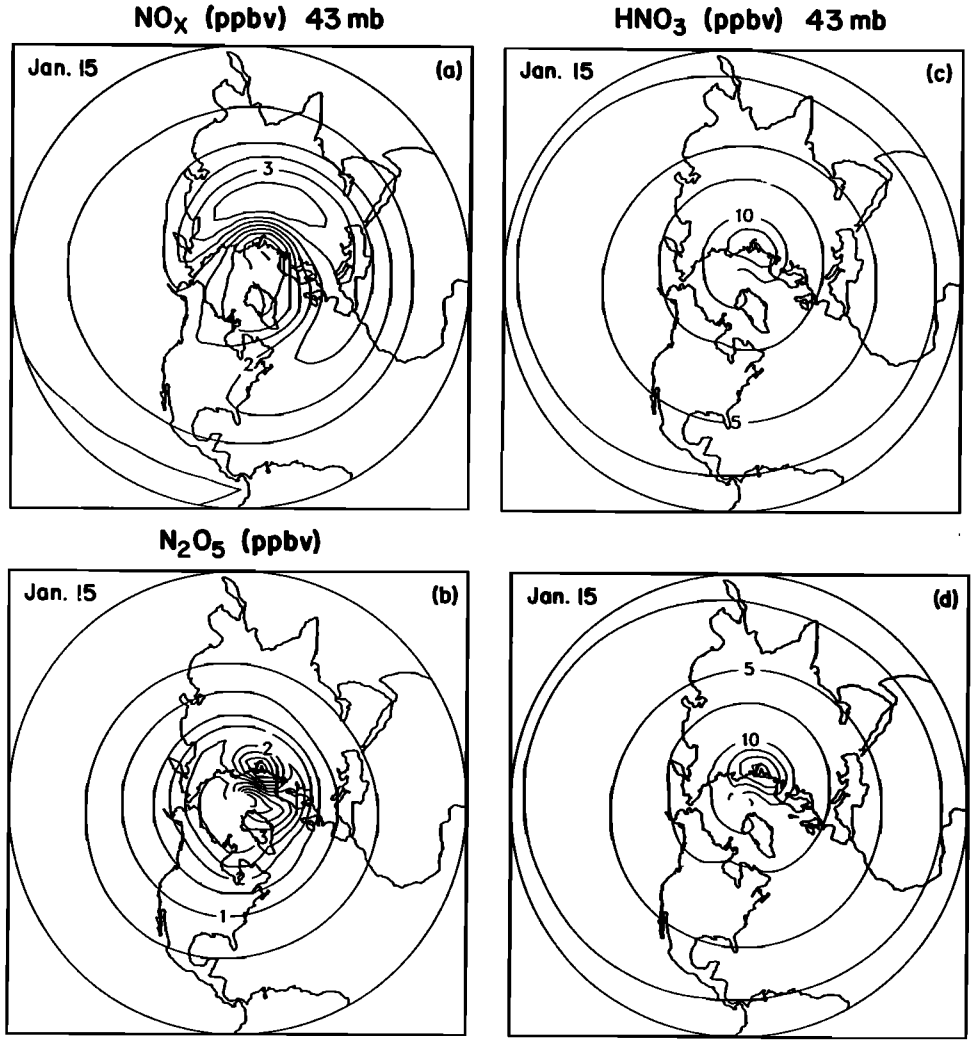

Fig. 13. Mixing ratio (ppbv) in the northern hemisphere (January 15) at 43 mbar of (*a*) NO_x, (*b*) N_2O_5, (*c*) HNO_3 (case 1N), and (*d*) HNO_3 (case 2N). Contour intervals: (*a* and *b*) 0.5 ppbv and (*c* and *d*) 2.5 ppbv.

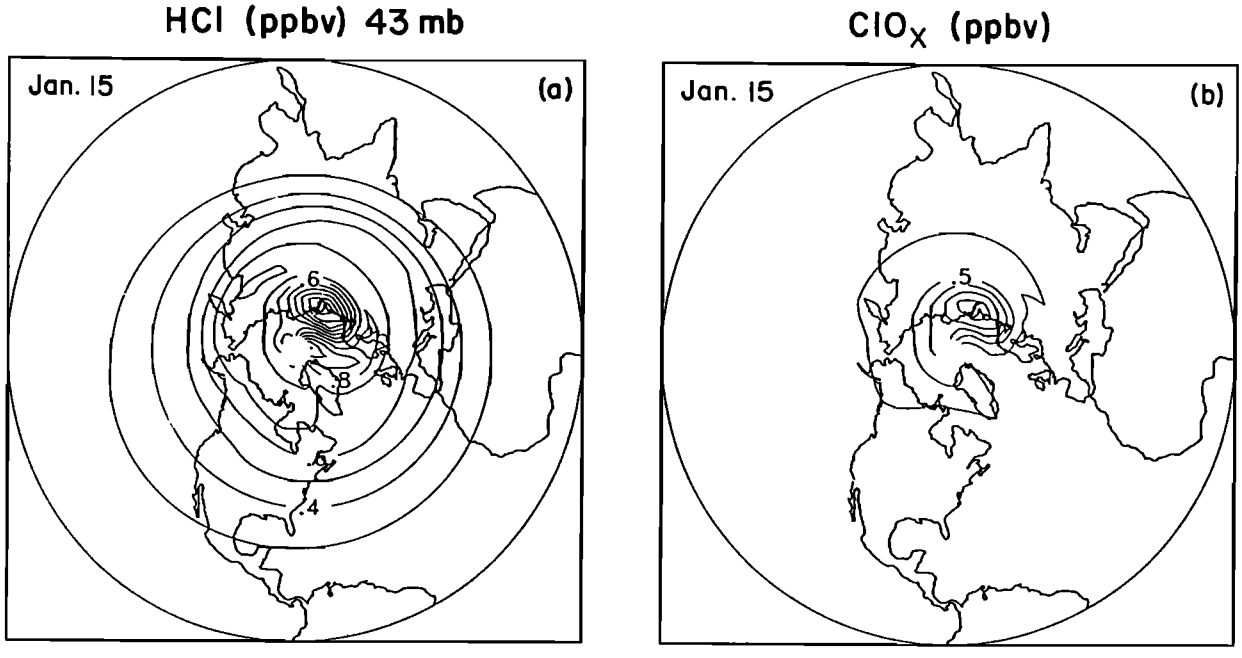

Fig. 14. Same as Figure 13 but for (*a*) HCl and (*b*) ClO_x. Contour intervals: (*a*) 0.1 ppbv and (*b*) 0.25 ppbv.

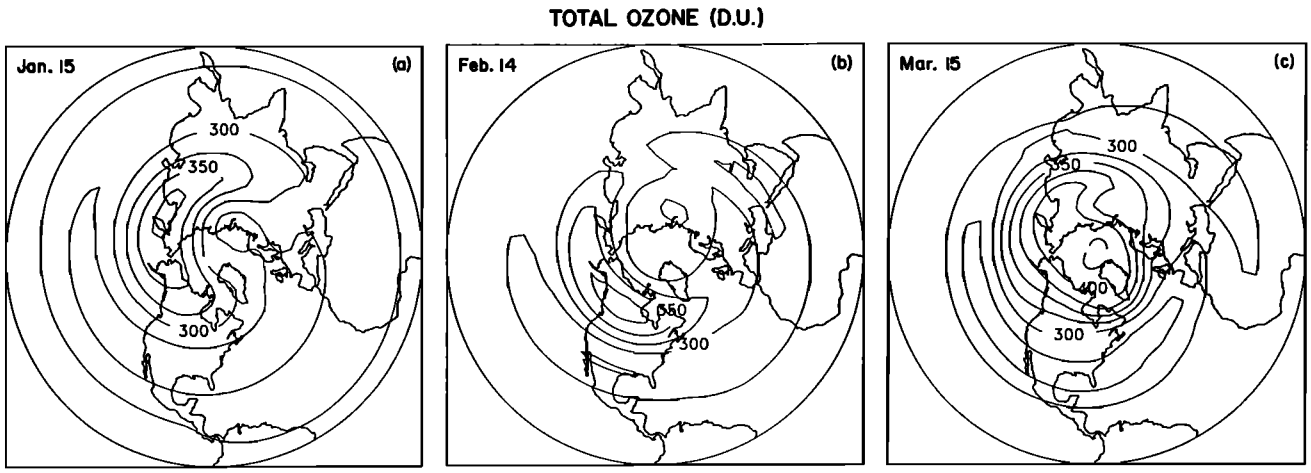

Fig. 15. Evolution of the ozone column abundance simulated in the northern hemisphere, (*a*) January 15, (*b*) February 14, and (*c*) March 15. Contour interval: 25 DU.

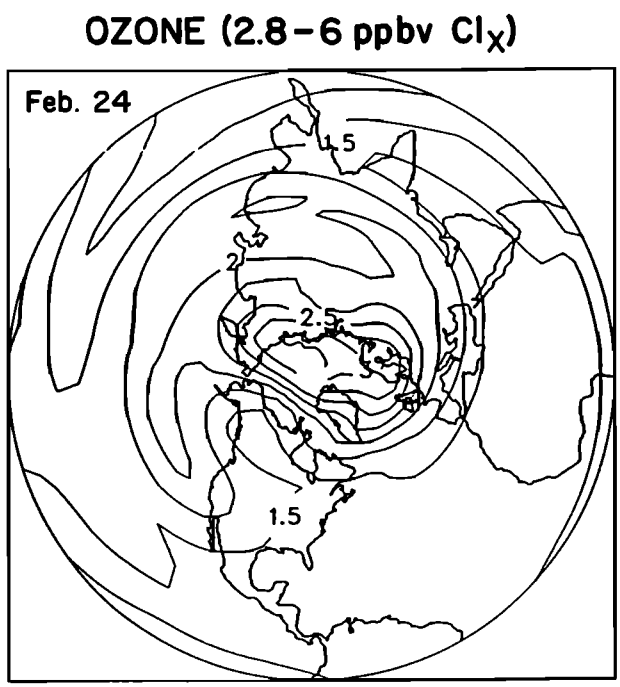

Fig. 16. Depletion in the ozone column (percent) in the northern hemisphere (February 24) calculated for an increase of Cl_X from 2.8 ppbv to 6.0 ppbv. Contour interval: 0.25%.

produce a substantial ozone depletion in the Arctic region. Figures 15*a*-15*c* show the evolution of the calculated ozone column abundance from January to March (case 1N). The ozone minimum, which is initially located over the pole, is displaced together with the vortex, while a maximum of ozone is determined in the warmer regions found at the edge of the polar region. The model produces strong fluctuations in the dynamical and ozone fields during the winter, but in March, after the final warming, the maximum in the ozone column (larger than 400 DU) is located near the pole. The model simulations clearly suggest that the difference in the ozone behavior in the Arctic and Antarctic results directly and indirectly from the different dynamical conditions. The Arctic vortex breaks up much earlier in the season than it does in Antarctica, so that mid-latitude ozone is transported by planetary waves towards the pole before much chemical destruction of O_3 can occur. In the model, the final warming in the northern hemisphere takes place in mid February. On the other hand, the temperature of the air masses are different in both hemispheres and consequently the chemistry is affected by hemispheric differences in the dynamics. The absence of an ozone hole in the northern hemisphere results from a lack of simultaneity between the presence of cold air masses and of solar radiation in the polar region.

An important question is to estimate the potential changes in the ozone abundance over the Arctic region in the future, when higher levels of chlorine will eventually be present in the atmosphere, as a result of chlorofluorocarbons emissions. To address this question again, a model simulation has been performed with a background chlorine concentration of 6 ppbv (case 4N). The results (February 24; see Figure 16) show reductions in ozone over the entire hemisphere (1.5% at mid-latitudes and 3% at high latitudes) but no ozone hole is produced during the entire model integration. Again, in contrast to what is seen in the southern hemisphere, this behavior of ozone in the northern hemisphere is governed by the timing of the final warming, which takes place before significant amounts of ozone have been destroyed. It should be emphasized, however, that a delay in the occurrence of the final warming from currently observed situations could eventually produce substantial ozone depletion at high latitudes in the northern hemisphere. Note that the ozone reduction calculated a mid and low latitudes is smaller than in most 2D model predictions. This difference is due to the limited time period during which the model was integrated (the initial ozone distributions are identical in both cases) and to the fact that it does not account for temperature feedbacks.

4. Discussion and Conclusions

In this study, we have shown that a 3D model with calculated transport and chemistry can quantitatively simulate the formation of a springtime ozone hole in Antarctica, when the model includes a simple but realistic description of polar

chemistry. With the same chemistry and the same initial conditions for the trace gases in both hemispheres but different dynamical forcings, the behavior of ozone is very different at high latitudes: no ozone hole is produced in the northern hemisphere, even with elevated chlorine levels.

The behavior of important chemical constituents is in relatively good agreement with observations made during polar campaigns in both hemispheres. The wintertime mixing ratio of water vapor in the lower stratosphere is reduced from 3.5 ppmv to about 1 ppmv over Antarctica but remains to its standard value of 3.5 ppmv in the Arctic. Nitrogen oxides are converted to nitric acid in both polar regions but the HNO_3 mixing ratio remains moderately elevated only in the Arctic, where limited denitrification takes place; in Antarctica, nitric acid is rapidly removed from the atmosphere through sedimentation of PSCs II particles. In the two polar regions, the chlorine reservoirs are transformed into active chlorine but in the Arctic, because of the relatively higher levels of odd nitrogen after the return of the Sun, a fraction of ClO is reconverted into the $ClONO_2$ reservoir; in Antarctica, because of strong denitrification, very little $ClONO_2$ is formed in early spring and the chemical destruction rate of ozone is higher than in the warmer Arctic. Figures 17*a*–17*c* show the latitudinal variation in the mixing ratio of various species calculated in

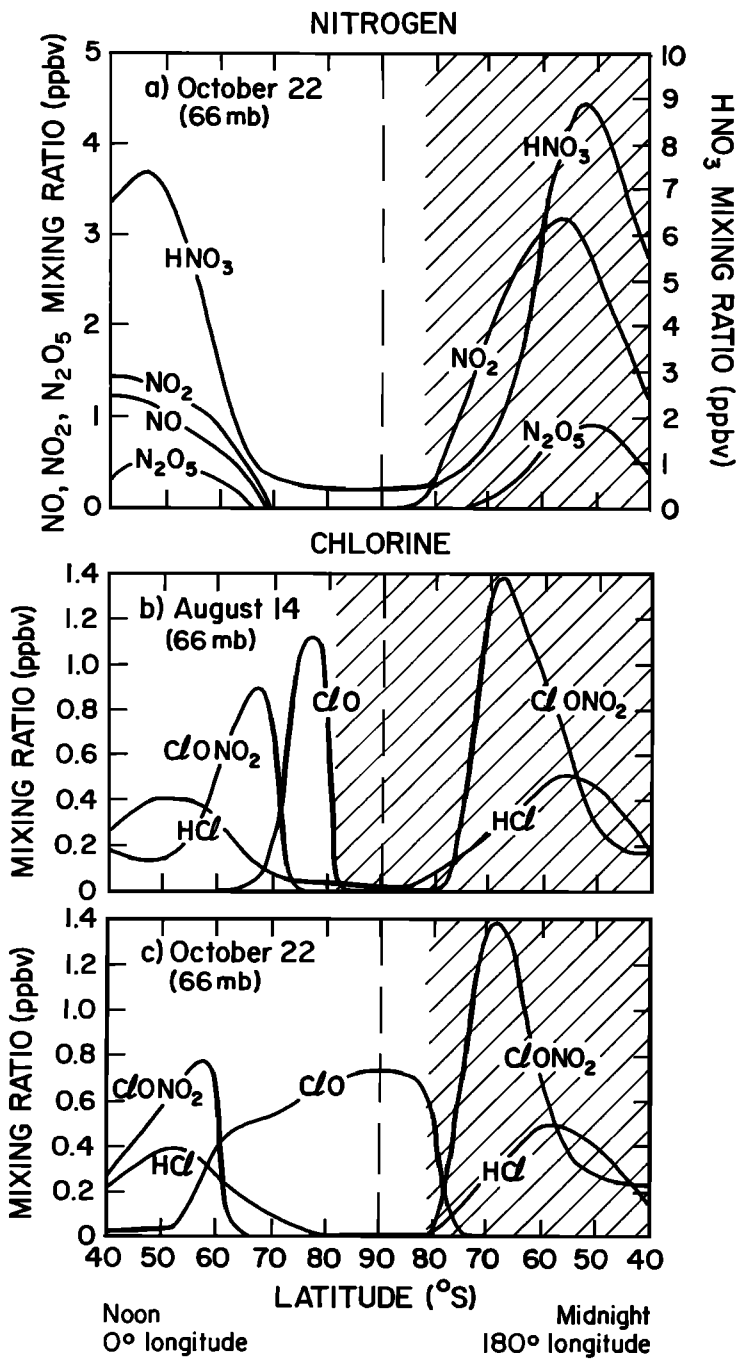

Fig. 17. Distribution at 66 mbar as a function of latitude for two longitudes (Greenwich meridian at noon and international date line at midnight) of (*a*) odd nitrogen species on October 22, (*b*) odd chlorine species on August 14, and (*c*) odd chlorine species on October 22.

the southern hemisphere at the 66 mbar level for noon and midnight conditions.

In the case of the odd nitrogen species, shown in Figure 17*a* for October 22, very low mixing ratios are seen in the region where polar stratospheric clouds are assumed to be present. Outside the vortex, the nitric acid concentration reaches a maximum near 55°N, which is slightly higher at 180° longitude (9 ppbv) than at 0° longitude (7.5 ppbv), as a result of the wave structure on this particular day. In the case of the oxides of nitrogen, the values of the calculated mixing ratios on both longitudes are to a large extent governed by the diurnal variation driven by solar insolation. In particular, NO which is present in the sunlit portion of the atmosphere, has been converted into NO_2 in the dark region.

The concentration of the species belonging to the chlorine family exhibits large latitudinal variation in the vicinity of the vortex (Figures 17*b* and 17*c*). Inside the vortex the mixing ratios of HCl and $ClONO_2$ are extremely low and ClO is present in large quantity only in the region illuminated by the Sun. In the inner region of the vortex, which is not illuminated, most of the chlorine is in the form of Cl_2O_2 (not shown). The region with large ClO mixing ratios (of the order of 1 ppbv) is therefore very narrow in mid-August (Figure 17*b*) but gradually increases in the subsequent weeks. In October (Figure 17*c*), elevated ClO densities are present over the South Pole at all times of the day. The mixing ratio of $ClONO_2$ reaches a maximum at the edge of the vortex (~65°S) and that of HCl is largest near 55°S.

The dynamics of both hemispheres are significantly different. In the southern hemisphere, the cold airmass, in which the perturbed chemistry takes place, remains located over the pole, while the warm air parcels move clockwise around the cold and isolated airmass trapped inside the polar vortex. In the northern hemisphere, the dynamical fields are significantly more disturbed by vertically propagating planetary waves and the polar vortex with its relatively cold air is often displaced from the pole. The model shows several other interesting features related to the dynamics of the stratosphere; for example, as time evolves, an oscillation in the amplitudes of the planetary waves in the southern hemisphere and an energy transfer between wave number 1 and 2 occurs, with a period of about 10 days. The role of the vortex as a material entity which isolates cold airmasses in both polar regions as well as the the transport of ozone from the subtropics to the polar region in the northern hemisphere are qualitatively well simulated by the model [*Rose*, 1986; *Rose and Brasseur*, 1989].

Several problems in the simulation should, however, be noted. The first and probably the most important of them is related to the coarse resolution of the grid on which the equations are solved. Despite the inclusion in the dynamical equations of the nonlinear terms, the cascade of energy from the largest to the smallest scales is limited to about wave number 4 and irreversible mixing to smaller scales is not explicitly calculated. A certain amount of mixing, however, is produced by the numerical filters applied to the model [*Rose and Brasseur*, 1989]. The breakdown of the vortex and the related dilution of the ozone hole are intimately related to processes on these small scales. Another problem for which small scales processes could be important is the fate of denitrified and dehydrated air after the final warming. It is still poorly understood how nitrogen oxides and water vapor are transported back into the Antarctic polar region and what role the chemistry of NO_x plays during this period. Only high-resolution dynamical/chemical models will be able to answer these questions. Finally, the degree of isolation of the polar vortex remains a matter of debate [*Hartmann et al.*, 1989; *Tuck*, 1989; *McKenna et al.*, 1989], and again, this problem requires calculations and data analyses made at high resolution.

An important and yet unsolved question is the strength of the vertical transport inside the polar vortices. Observational data based on the measurement of long-lived trace gases such as the chlorofluorocarbons, methane or nitrous oxides, suggest that substantial downward transport takes place before spring [*Loewenstein et al.*, 1989; *Heidt et al.*, 1989; *Toon et al.*, 1989]. *Toon et al.* [1989] found, for example, that over the Antarctic station of McMurdo the vertical distribution of long-lived species measured in spring is translated downwards by some 6–8 km relative to airmasses outside the vortex. The measurements of *Mankin et al.* [1990] made over the North Atlantic in January 1989 during an Arctic campaign suggest a similar vertical translation of about 6 km with respect to those outside. The model calculates the distribution of methane. The mixing ratios at high latitudes (see Figure 18) in the southern hemisphere are the lowest in the polar region but they do not exhibit the type of sharp gradient that is observed at the edge of the vortex. The dynamics before or during the winter season may precondition the distribution of the quasi-inert tracers inside and outside the vortex. A simulation of these processes requires simulations to be performed over an entire year as opposed to 4 months as in this study. Also, the evolution in time of the tropospheric forcing and the role of radiative processes for vertical motions inside the vortex need to be treated in more detail than in the present model.

Another limitation of the model (which weakens its prediction capability) results from the assumption concerning the removal of odd nitrogen from the gas phase inside the polar vortex. It has been shown that the ozone loss in this region is significantly affected by the degree of denitrification. This latter quantity should be determined by a detailed microphysical cloud model.

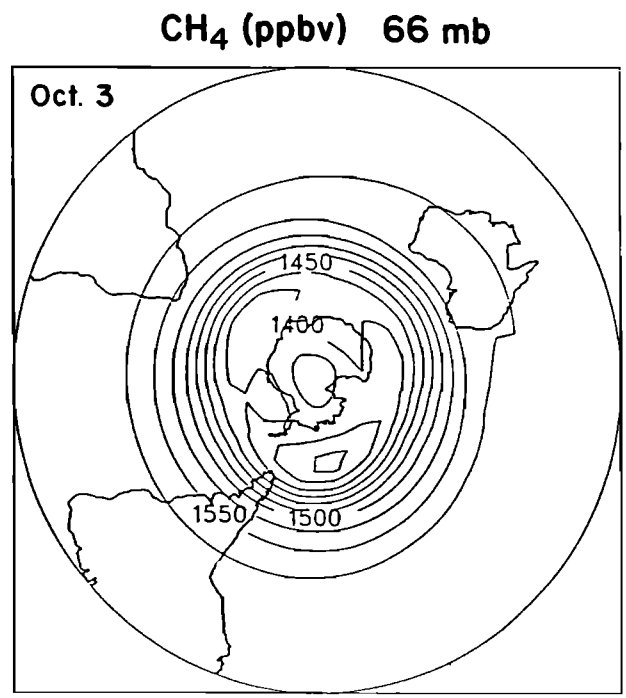

Fig. 18. Mixing ratio (ppbv) of methane on the 66 mbar surface on October 3 in the southern hemisphere. Contour interval: 25 ppbv.

Despite the simplifications associated with this model, important features observed during the Antarctic and Arctic campaigns are reproduced. Information about the relative roles of chemistry and dynamics in the formation of the ozone hole is provided and should contribute to the interpretation of numerous data collected during recent years in both polar regions. Finally, the model gives some insight about the future changes in polar ozone, if the level of chlorine continues to increase in the atmosphere. It should be added, however, that a more reliable prediction would be achieved if dynamical (radiative) feedback as well as the still poorly understood role of background sulfuric acid aerosols on the high latitude ozone chemistry were taken into account.

Acknowledgments. We dedicate this paper to Klaus Rose, who died in December 1989 and who had developed at the Free University of Berlin the dynamical model used in this work. We are grateful to R. Garcia and W. Mankin for valuable comments on the manuscript. We acknowledge with thanks the contribution of S. Walters and D. Middleton for programming support, and D. Sanerib for typing the manuscript. Claire Granier is on leave from CNRS, France, and is supported by a grant from the European Space Agency (ESA External Fellowship Program). The National Center for Atmospheric Research is sponsored by the National Science Foundation.

REFERENCES

Anderson, J. G., W. H. Brune, M. J. Proffitt, W. Starr, and K. R. Chan, In situ observations of ClO in the Antarctic: Evidence for chlorine catalyzed destruction of ozone, Polar Ozone Workshop, *NASA Conf. Publ., 10014*, 1988.

Anderson, J. G., W. H. Brune, and M. H. Proffitt, Ozone destruction by chlorine radicals within the Antarctic vortex: The spatial and temporal evolution of ClO-O_3 anticorrelation based on in situ ER-2 data, *J. Geophys. Res., 94*, 11,465–11,479, 1989*a*.

Anderson, J. G., W. H. Brune, S. A. Lloyd, D. W. Toohey, S. P. Sander, W. L. Starr, M. Loewenstein, and J. R. Podolske, Kinetics of O_3 destruction by ClO and BrO within the Antarctic vortex: An analysis based on in situ ER-2 data, *J. Geophys. Res., 94*, 11,480–11,520, 1989*b*.

Austin, J., R. L. Jones, D. S. McKenna, A. T. Buckland, J. G. Anderson, D. W. Fahey, C. B. Farmer, L. E. Heidt, M. H. Proffitt, A. F. Tuck, and J. F. Vedder, Lagrangian photochemical modeling studies of the 1987 Antarctic spring vortex, 2, Seasonal trends in ozone, *J. Geophys. Res., 94*, 16,717–16,735, 1989.

Brasseur, G., and P. C. Simon, Stratospheric chemical and thermal response to long-term variability in solar UV irradiance, *J. Geophys. Res., 86*, 7343–7362, 1981.

Brasseur, G., and S. Solomon, *Aeronomy of the Middle Atmosphere*, 452 pp., D. Reidel, Hingham, Mass., 1986.

Brasseur, G., M. H. Hitchman, S. Walters, M. Dymek, E. Falise, and M. Pirre, An interactive chemical dynamical radiative two-dimensional model of the middle atmosphere, *J. Geophys. Res., 95*, 5639–5655,1990.

Brühl, C., and P. J. Crutzen, The potential role of odd hydrogen in the ozone hole photochemistry, in *Our Changing Atmosphere*, edited by P. J. Crutzen, J. C. Gérard and R. Zander, Proceedings of the 28th Liège International Astrophysical Colloquium, University of Liège, Belgium, 1990.

Cariolle, D., A. Lasserre-Bigorry, J.-F. Royer, and J.-F. Geleyn, A general circulation model simulation of the springtime Antarctic ozone decrease and its impact on mid-latitudes, *J. Geophys. Res., 95*, 1881–1898, 1990.

DeMore, W. B., M. J. Molina, S. P. Sander, D. M. Golden, R. F. Hampson, M. J. Kurylo, C. J. Howard, and A. R. Ravishankara, Chemical kinetics and photochemical data for use in stratospheric modeling, Evaluation Number 8, *JPL Publ.*, 87–41, 1987.

Dickinson, R. E., Method of parameterization for infrared cooling between altitudes of 30 and 70 kilometers, *J. Geophys. Res., 78*, 4451–4457, 1973.

Dobson, G. M. B., Origin and distribution of polyatomic molecules in the atmosphere, *Proc. R. Soc. London, Ser. A, 236*, 187–193, 1956.

Douglass, A. R., and R. S. Stolarski, Impact of heterogeneous reactions on stratospheric chemistry in the Arctic, *Geophys. Res. Lett., 16*, 131–134 1989.

Fahey, D. W., K. K. Kelly, G. V. Ferry, L. R. Poole, J. C. Wilson, D. M. Murphy, M. Loewenstein, and K. R. Chan, In situ measurements of total reactive nitrogen, total water and aerosol in a polar stratospheric cloud in the Antarctic, *J. Geophys. Res., 94*, 11,299–11,315, 1989.

Farman, J. C., B. G. Gardiner, and J. D. Shanklin, Large losses of total ozone over Antarctica reveal seasonal ClO_x/NO_x interactions, *Nature, 315*, 207–210, 1985.

Gandrud, B. W., P. D. Sperry, L. Sanford, K. K. Kelly, A. V. Ferry, and K. R. Chan, Filter measurements from the Airborne Antarctic Ozone Experiment, *J. Geophys. Res., 94*, 11,285–11,286, 1989.

Hartmann, D. L., K. R. Chan, B. L. Gary, M. R. Schoeberl, P. A. Newman, R. L. Martin, M. Loewenstein, J. R. Podolske, and S. E. Strahan, Potential vorticity and mixing in the south Polar vortex during spring, *J. Geophys. Res., 94*, 11,625–11,640, 1989.

Heidt, L. E., J. F. Vedder, W. H. Pollock, R. A. Lueb, and B. E. Henry, Trace gases in the Antarctic atmosphere, *J. Geophys. Res., 94*, 11,599–11,611, 1989.

Henderson, G. C., F. J. Evans, and J. C. McConnell, Effects of initial active chlorine concentrations on the Antarctic ozone spring depletion, *J. Geophys. Res., 95*, 1899–1908, 1990.

Hofmann, D. J., J. W. Harder, S. R. Rolf, and J. M. Rosen, Balloon-borne observations of the temporal development and vertical structure of the Antarctic ozone hole in 1986, *Nature, 326*, 59–62, 1987.

Jones, R. L., J. Austin, D. S. McKenna, J. G. Anderson, D. W. Fahey, C. B. Farmer, L. E. Heidt, K. K. Kelly, D. M. Murphy, M. H. Proffitt, and A. F. Tuck, Lagrangian photochemical modeling studies in the 1987 Antarctic spring vortex, 1, Comparison with observations, *J. Geophys. Res., 94*, 11,529–11,558, 1989.

Kelly, K. K., A. F. Tuck, D. M. Murphy, M. H. Proffitt, D. W. Fahey, R. L. Jones, D. S. McKenna, M. Loewenstein, J. R. Podolske, S. E. Strahan, A. V. Ferry, K. R. Chan, J. F. Vedder, G. L. Gregory, W. D. Hypes, M. P. McCormick, E. V. Browell, and L. E. Heidt, Dehydration in the lower Antarctic stratosphere during late winter and early spring, 1987, *J. Geophys. Res., 94*, 11,317–11,357, 1989.

Kiehl, J. T., B. A. Boville, and B. P. Briegleb, Response of a general circulation model to a prescribed Antarctic ozone hole, *Nature, 332*, 501–504, 1988.

Krueger A. J., M. S. Schoeberl, S. D. Doiron, F. Sechrist, and R. Galimore, Total ozone changes in the 1987 Antarctic ozone hole, Polar Ozone Workshop, *NASA Conf. Publ., 10014*, 1988.

Leu, M. T., Heterogeneous reactions of N_2O_5 with H_2O and HCl on ice surfaces: Implications for Antarctic ozone depletion, *Geophys. Res. Lett., 15*, 855–858, 1988.

Loewenstein, M., J. R. Podolske, K. R. Chan, and S. E. Strahan, Nitrous oxide as a dynamical tracer in the 1987 Airborne Antarctic Ozone Experiment, *J. Geophys. Res., 94*, 11,589–11,598, 1989.

London, J., Radiative energy sources and sinks in the stratosphere and mesosphere, in *Proc. NATO Advanced Study Institute, Atmospheric Ozone: Its Variation and Human Influences*, pp. 703–721, U.S. Dep. of Transportation, Washington, D. C., 1980.

Mankin, W. G., M. T. Coffey, A. Goldman, M. R. Schoeberl, L. R. Lait, and P. A. Newman, Airborne measurements of stratospheric constituents over the Arctic in the winter of 1989, *Geophys. Res. Lett., 17*, 473, 1990.

McCormick, M. P., and C. R. Trepte, SAM II measurements of Antarctic PSCs and aerosols, *Geophys. Res. Lett., 13*, 1276–1279, 1986.

McCormick, M. P., and C. R. Trepte, Polar stratospheric optical depth observed between 1978 and 1985, *J. Geophys. Res., 92*, 4297–4306, 1987.

McCormick, M. P., C. R. Trepte, and M. C. Pitts, Persistence of polar stratospheric clouds in the southern polar region, *J. Geophys. Res., 94*, 11,241–11,251, 1989.

McElroy, M. B., R. J. Salawitch, S. C. Wofsy, and J. A. Logan, Antarctic ozone: Reductions due to synergistic interactions of chlorine and bromine, *Nature, 321*, 759–762, 1986.

McKenna, D. S., R. L. Jones, J. Austin, E. V. Browell, M. P. McCormick, A. J. Krueger, and A. F. Tuck, Diagnostic studies of the Antarctic vortex during the 1987 Airborne Antarctic Ozone Experiment: Ozone miniholes, *J. Geophys. Res., 94*, 11,641-11,668, 1989.

Molina, L. T., and M. J. Molina, Production of Cl_2O_2 from the self

reaction of the ClO radical, *J. Phys. Chem., 91*, 433–436, 1987.
Molina, M. J., T. L. Tso, L. T. Molina, and F. C. Y. Wang, Antarctic stratospheric chemistry of chlorine nitrate, hydrogen chloride, and ice: Release of active chlorine, *Science, 238*, 1253–1257, 1987.
Poole, L. R., and M. P. McCormick, Airborne lidar observation of Arctic polar stratospheric clouds: Indications of two distinct growth modes, *Geophys. Res. Lett., 15*, 21–23, 1988.
Prather, M., M. M. Garcia, R. Suozzo, and D. Rind, Global impact of the Antarctic ozone hole: Dynamical dilution with a three-dimensional chemical transport model, *J. Geophys. Res., 95*, 3449–3472, 1990.
Proffitt, M. H., J. A. Powell, A. F. Tuck, D. W. Fahey, K. K. Kelly, M. Loewenstein, J. R. Podolske, and K. R. Chan, Temporal trends and transport within and around the Antarctic polar vortex during the formation of the 1987 Antarctic ozone hole, Polar Ozone Workshop, *NASA Conf. Publ., 10014*, 1988.
Ramaswamy, V., Dehydration mechanism in the Antarctic stratosphere during winter, *Geophys. Res. Lett., 15*, 863–866, 1988.
Randel, W. J., Global atmospheric circulation statistics 100–1 mb, *NCAR Tech. Note, NCAR/TN-295+STR*, 1987.
Randel, W. J., The seasonal evolution of planetary waves in the southern hemisphere stratosphere and troposphere, *Q. J. R. Meteorol. Soc., 114*, 1385–1409, 1988.
Rodriguez, J. M., M. K. W. Ko, and N. D. Sze, Chlorine chemistry in the Antarctic stratosphere: Impact of OClO and Cl_2O_2 and implications for observations, *Geophys. Res. Lett., 13*, 1292–1295, 1986.
Rose, K., On the influence of nonlinear wave-wave interaction in a 3-D primitive equation model for sudden stratospheric warming, *Beitr. Phys. Atmos., 56*, 14–41, 1983.
Rose, K., The stratospheric winter polar vortex simulated as a material entity, *J. Atmos. Terr. Phys., 48*, 1197–1202, 1986.
Rose, K., and G. Brasseur, A three-dimensional model of chemically active trace species in the middle atmosphere during disturbed winter conditions, *J. Geophys. Res., 94*, 16,387–16,403, 1989.
Salawitch, R. J., S. C. Wofsy, and M. B. McElroy, Chemistry of OClO in the Antarctic stratosphere: Implications for bromine, *Planet. Space Sci., 36*, 213–224, 1988.
Sander, S. P., R. R. Friedl, Y. L. Yung, Rate of formation of the ClO dimer in the polar stratosphere; implications for ozone loss, *Science, 245*, 1095–1098, 1989.
Shiotani, M., and J. C. Gille, Dynamical factors affecting ozone mixing ratios in the Antarctic lower stratosphere, *J. Geophys. Res., 92*, 9811–9824, 1987.
Solomon, S., R. R. Garcia, F. S. Rowland, and D. J. Wuebbles, On the depletion of Antarctic ozone, *Nature, 321*, 755–758, 1986.
Solomon, S. R. W. Sanders, M. A. Carroll, and A. L. Schmeltekopf, Visible and near-ultraviolet spectroscopy at McMurdo Station, Antarctica, 6, Observations of the diurnal variations of BrO and OClO, *J. Geophys. Res., 94*, 11,393–11,403, 1989.
Stolarski, R. S., A. J. Krueger, M. R. Schoeberl, R. D. McPeters, P. A. Newman, and J. C. Alpert, NIMBUS 7 SBUV/TOMS measurements of the springtime Antarctic ozone hole, *Nature, 322*, 808–811, 1986.
Sze, N. D., M. K. W. Ko, D. K. Weisenstein, J. M. Rodriguez, R. S. Stolarski, and M. R. Schoeberl, Antarctic ozone hole: Possible implications for ozone trends in the southern hemisphere, *J. Geophys. Res., 94*, 11,521–11,528, 1989.
Tolbert, M. A., M. J. Rossi, R. Malhotia, and D. M. Golden, Reaction of chlorine nitrate with hydrogen chloride and water at Antarctic stratospheric temperatures, *Science, 238*, 1258–1260, 1987.
Toon, G. C., C. B. Farmer, P. W. Schaper, J.-F. Blavier, and L. L. Lowes, Ground-based infrared measurements of tropospheric source gases over Antarctica during the 1986 austral spring, *J. Geophys. Res., 94*, 11,613–11,624, 1989.
Toon, O. B., P. Hamill, R. P. Turco, and J. Pinto, Condensation of HNO_3 and HCl in the winter polar stratosphere, *Geophys. Res. Lett., 13*, 1284–1287, 1986.
Tuck, A. F., Synoptic and chemical evolution of the Antarctic vortex in late winter and early spring, 1987, *J. Geophys. Res., 94*, 11,687–11,737, 1989.
Turco, R. P., O. B. Toon, and P. Hamill, Heterogeneous physicochemistry of the polar ozone hole, *J. Geophys. Res., 94*, 16,493–16,510, 1989.
United National Environment Program and World Meteorological Organization, *Scientific Assessment of Stratospheric Ozone: 1989*, Vol. I, WMO/Global Ozone Research and Monitoring Project, Report No. 20, 486 pp., Geneva, 1990.

G. Brasseur, National Center for Atmospheric Research, P. O. Box 3000, Boulder, CO 80307.
C. Granier, Service d'Aeronomie, Centre National de la Recherche Scientifique, Paris, France.

(Received April 6, 1990;
revised August 2, 1990;
accepted August 8, 1990.)